TECHNIUM

Technium Vol. 3, Issue 3 pp.41-52 (2021)
ISSN: 2668-778X
www.techniumscience.com

Synergistic effect of chromium on the mechanical properties and microstructures of spheroidal graphite cast iron

Mulaja Tshakatumba Constantin[1*], Moramess Ngoy Moses Raphael[1], Tshipeshi Makina Héritier[1], Kiswakala Katwebe Kaki Jospin[1], Kyungu Mutumba Dieudonné[2], Nkulu Wa Ngoie Guy[1].

[1]Metallography and Materials, Metallurgy, Polytechnics, University of Lubumbashi, DRC
[2]Central Panda Workshops (ACP/Gecamines), Likasi, DRC

[*]Corresponding author e-mail: tshaka021@yahoo.fr

Abstract. The fragmentation equipment used in ore's preparation operations is internally lined with armor whose characteristics require better wear resistance and resilience. The aim of this study was to develop a new generation of high-performance 4% Cr spheroidal graphite (GS) cast iron materials for the manufacture of self-growing shredder lift bars. This typeface was designed in the optic to replace the commonly used white cast iron. The results were used to assess the effect of chromium on the microstructure of the cast iron as well as on its mechanical behavior. It is noted that the presence of chromium leads to the appearance of eutectic carbides and out-of-balance dies. Two types of chromium carbide $(Fe,Cr)_7C_3$ and $(Fe,Cr)_3C$ precipitate into the matrix and effectively contribute to the improvement of mechanical performances of this material.The quench and tempering heat treatments applied to these materialsled to the following optimum values: impact resistance of 4.8 J/cm^2 for the GS 4Cr nuance, 5 J/cm^2 for the GS nuance and 0.9 J/cm^2 for the 9 cast iron nuance; hardness values of 691, 511 and 509 HV30 were measured respectively for GS 4Cr cast iron, GS cast iron and 9 cast iron treated. The optimal lifetime of each material was estimated at approximately 285 days for treated GS cast iron, 585 days for GS 4Cr cast iron treated and 242 days for normalized cast iron 9.
Keywords: Synergic, cast iron, spheroidal graphite, wear, materials lifetime

1. Introduction

Lift bars are important pieces in the composition of a grinder [1].However, they undergo frequent wear which, in some cases, lead to breakage. This is the result of the force exerted by abrasive products such as minerals and grinding bodies, particularly during a grinding operation[2] [3] [4] [5] [6].The good material's choice must simultaneously meet the excellent wear and impact resistance requirements.Allied white cast irons represent a promising class materials for making these pieces [1] [7] [8].The 9 cast iron nuance (F9) made at the Gecamines' Central Workshops is the one commonly used for this purpose in the mining sphere of Great Katanga. In addition to its better resistance to wear due in particular to its chromium content (18-28% Cr), this shade has low resistance to shocks with a near-zero value [1][7][9]. This significantly affects the productivity of a grinding circuit in minerals preparation.

This study was initiated with the main target of substituting the 9 cast iron currently produced in Central Panda Workshops ACP, with a nuance that can combine the best wear and impact resistance

properties. For this purpose, the choice was made on the spheroidal graphite cast iron optimized by addition of chromium [1][7][9][10] [11][12][13].

2. Materials and Methods

2.1. Materials

In this study, several raw materials were used in the manufacture of spheroidal graphite cast iron, namely: cast iron scrap containing 1.95% silicon, ferro-silico-magnesium (6% Mg, 42% Si) for spheroiding of graphite leading to GS cast iron,ferro-manganese HC(80% Mn), andferro-chromeH-VS(68% Cr) for obtainingGS cast iron.

The chemical composition of the materials was determined using a Bruker S2 PumaX-Ray FluorescenceSpectrometer. Carbon and sulfur levels were determined at ELTRA's ELEMENTRAC CS-i carbo-sulphometer (Carbon Sulfur Determinator).Table 1 shows the averages of the five of those results during this analysis.

The elaboration of this typeface was conducted according to a Gecamines's standard specific. The fusion of the pig cast iron was carried out in a Birlec-branded single phase arc electric furnace with a capacity of 50 kg, the addition of elements has been done according to the chemical composition of each material.

The materials loaded in the furnace are brought to a temperature of around 1370°Cbefore addingferro-chrome HC(68% Cr) and then this molten material overheated to 1430°C before the addition of ferro-manganese HC(80% Mn) and ferro-silico-magnesium (6% Mg, 42% Si). An additional 20°C overheating is subjected to melting before it is poured into sand molds for the manufacture of various test tubes.

2.2. Heat treatment

A LINN HIGH THERM VMK 1600 electric mitten oven for thermal treatment operations. It should be noted that the GS and GS 4Cr cast irons underwent heat treatment following a austenization cycle at 960-degree during 1 hour followed by a quench in water and a tempering at 275°C for 1 hour followed by cooling in the oven. This tempering heat treatment is realized with the aim of transforming quenched martensite into a tempering martensite while reducing internal constraints due to quench heat treatment. Cast iron 9, on the other hand, underwent a normalization heat treatment starting at 950 ° C for 30 minutes followed by air cooling [14].

2.3. Mechanical tests

2.3.1. Hardness test

The Vickers hardness measurement was performed on the flat surface of the previously prepared cross section. The measurement was made with an AFFRI OMAG Vickers durometer equipped with a camera attached to a computer. The load used was 30 kgf according to the standard ASTM_E140_T3.The HV30 values were obtained within a radius from the periphery to the core of the materials. The samples were previously polished without the slightest chemical attack. Six hardness measurements were performed on each sample and the hardness of the material consisting of the arithmetic mean has been calculated and converted.

2.3.2. Impact test

The impact test was performed on a prepared test tube, according to ASTEM E 23-96, whose dimensions were: 55 mm in length, 100 mm^2 square section and 0.2 mm deep V-shaped notch.

The measurement was made with a semi-automatic Charpy pendelum impact test brand PSW 360. Impact resistance was calculated from the energy stored by the test tube and the surface of the test tube.

2.3.3. Abrasion wear test

The wear tests were carried out using a FORCIPOL 1V disc polisher rotating at a speed of 300 rpm on which are attached an abrasive paper (P80) and a sample in abrasion wear mode for 2 min with a force of about 18 N. Mass losses were assessed for each shade.

Wear resistance was quantified as a percentage by the Micro-Deval Coefficient (CMD) ie:

$$CMD[\%] = \frac{100 * m}{M}$$

Where M is the sample mass tested and m the mass of elements less than 1.6 mm produced during the testaccordingtoNorm NF P 18 - 572.

2.4. Microstructural characterization

Thismetallographic characterizationwas performed, after polishing and attacking samples for 15 to 20 seconds with Nital4%, under the OPTIKA brand optical microscope equipped with a camera.

3. Results

3.1. Microstructural characterization

Chemical analysis results of samples are included in Table 1 below.With regard to chemical analysis results below presented, the high chromium content of F9 (high-chromium cast iron) portends the formation of a large quantity of eutectic and secondary carbides types in this material, leading to obtaining of increased hardness but also a fragility of the material. The presence of gammagenic elements such as Cu and Mn in considerable quantities ($\geq 0.5\%$) promote the formation of pearlite. But the very high content ofchromium (antigraphitis) would prevent the formation of graphite.

Table 1 - Chemical Composition of material nuances

%	F9	GS	GS 4Cr
VS	2.9	2.4	2.8
Cr	19	0.3	4.5
Yes	0.5	3.5	3.6
Cu	1	1	0.9
Mo	0.04	0.04	0.09
Mn	0.5	0.8	1.3
Mg	-	0.027	0.034
Or	1	0.7	0.5
S	0.1	0.01	0.03
P	0.1	1	-
Ti	-	0.1	0.9

The high silicon content and low enough chromium content in GS and GS 4Cr cast irons presages a graphitization of these cast irons thus leading to the expected mechanical performance with cheap materials. The presence of alloy elements such as Mo, Cu, Mn and Ni greatly influences the formation of microstructures of spheroid graphite cast irons : molybdenum ($\geq 0.05\%$) stabilizes the ferrite by increasing the temperature of the eutectoid and forms fine carbide within the metal matrix, Cu ($\geq 0.5\%$) promotes the formation of pearlite by delaying the diffusion of carbon within the austenite, manganese ($\geq 0.5\%$) promotes the formation of pearlite and stabilizes the austenite by reducing the eutectoid temperature and nickel ($\geq 0.5\%$) stabilizes the austenite by reducing the eutectoid

temperature, it promotes very slightly the formation of pearlite. Silicon, on the other hand, is ferritizing. The magnesium's presence at levelsr anging from 0.020 to 0.035% in cast iron with very low sulphur content ($\leq$ 0,05%)willlead to partial precipitation of vermicles graphite in a spheroidal graphite cast iron [15].

The metallographic results obtained are shown in figures 1, 2 and 3.

- The microstructure of this nuance presented in figure 1 shows the formation of a coarse ferrito-pearlitic matrix (figure 1 left) obtained by slow cooling in molds, graphite nodules and graphite vermicles obtained as a result of the ferro-silico-magnesium addition before casting, thus causing graphitization of carbon [15] [18]. The heat treatment of this nuance leads to the formation of a bainite coarse needles structure in austenitic-martensitic matrix accompanied by graphite nodules and vermicles (figure 1 right) obtained by rapid cooling of the material [12] [19] [20].
- Figure 2 (left) shows the formation of a fine ferrito-pearlitic matrix accompanied by nodules and graphite vermicles [15] [18]. The heat treatment applied to the material leads to precipitation of two kinds of carbides, the slats of eutectic carbides and fine type of secondary carbides$(Cr,Fe)_7C_3$ and $(Cr, Fe)_3$ Cin an austeno-martensitic matrix [12] [19] [20]; this also justifies the synergistic effect of the chromium addition on the material by the formation of two carbides each having a specific role. This structure gives this nuance intrinsic properties of hardness and rigidity with sufficient tenacity retention [9]. Graphite nodules are also present in the material reflecting the graphitization of carbon (figure 2 right).
- The microstructure of *9* cast iron nuance(figure 3) shows the precipitation of a proeutectoid carbide around aggregates of fine perlite with a transformed ledeburite after normalization heat treatment. The proeutectoid carbides are$(Cr,Fe)_7C_3$ and $(Cr,Fe)_{23}C_6$ types. The carbide $(Cr,Fe)_7C_3$ is a carbide rich in chromium which is formed when the chromium content is high enough compared to other alloying elements. The presence of molybdenum at a fairly low content leads to the formation of carbide $(Cr,Fe)_{23}C_6$. The presence of these two secondary carbides, particulary transformed ledeburite, gives the cast iron good intrinsic properties from the point of view of hardness and rigidity [21].

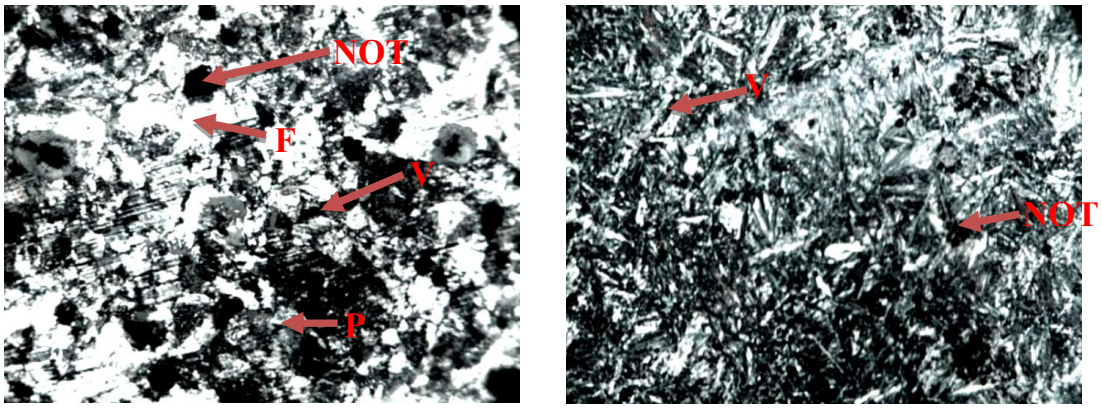

Figure 1 - Optical microscopy of cast iron GS nuance (Gr: 50x0.5): raw casting material (left) and after quench and tempering heat treatment (right)

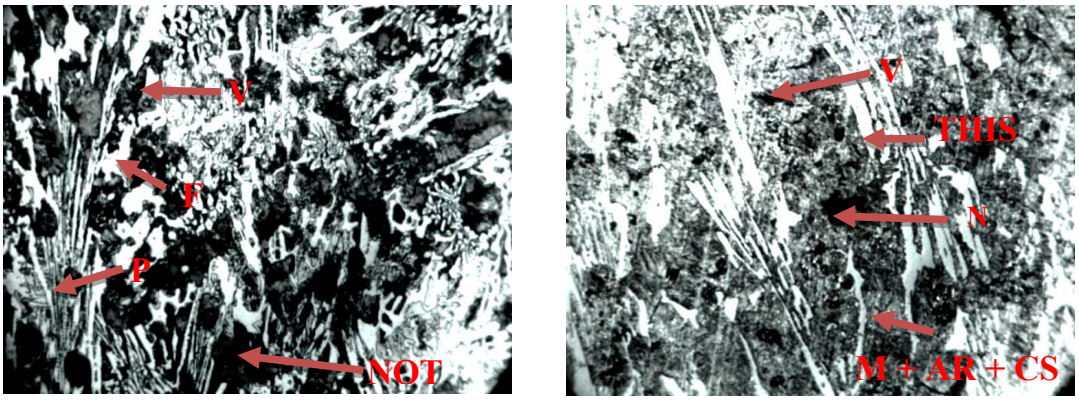

Figure 2 - Optical microscopy of cast iron GS 4Cr nuance: raw casting material (left, Gr: 12x20) and and after quench and tempering heat treatment (right, Gr: 50x0.5)

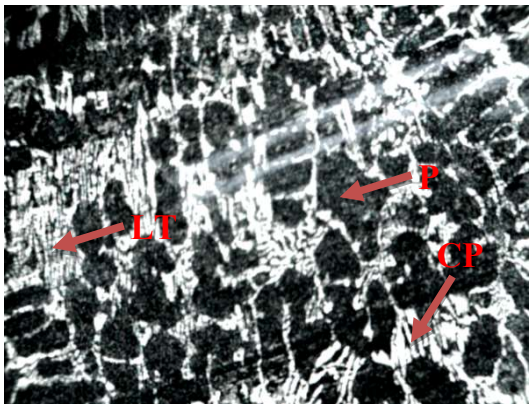

Figure 3 - Optical microscopy of cast iron 9 normalized (Gr: 50x0.5)

Caption:

B: Bainite
F: Ferrite
M: Martensite
N: Nodule
P: Pearlite
V: Vermicle
AR: Residual Austenite
CE: Eutectic Carbide
CP: Proeutectoid Carbide
CS: Secondary Carbide
LT: Transformed Ledeburite

3.2. Hardness of materials

The results of these tests are presented in tables 2 and 3.

3.2.1 Raw casting materials

In table 2, which contains untreated materials, there is a discrepancy between the hardness values obtained on the three naunces of cast iron. The hearts of these materials have high hardness relative to the periphery. In the raw casting state, the GS 4Cr cast iron nuance has the highest average hardness of all (554 HV30). The low hardness value of the GS cast iron compared to other nuances could be explained by the very small amount of chrome in the unalloyed GS cast iron; because chromium is a carburigenic element (antigraphitis) and is likely to form with the carbon present carbides having a hardening effect [16].

The GS 4Cr nuance has a higher hardness compared to that of cast 9. This could be explained by the installation of chromium atoms as a solid solution by substitution in the iron network causing a hardening by effect of solid solution. To this is added the synergistic effect of two carbides formed by the presence of sufficient amounts of chromium in the material. Chromium, for its carburigenic

character, is likely to form with the present carbon carbides with a hardening effect of The Shape Cr_7C_3 and Cr_3C [16].

3.2.2.Treated materials

After quench and tempering heat treatment, results in table 2 show that the GS and GS 4Cr nuances have high hardness values. However, the GS 4Cr is still the highest average of all (691 HV30). Nevertheless, the GS cast iron nuance has, after thermal treatment, an average of hardness now higher than that of nuance 9.

This could be explained by the fact that quench heat treatment applied has allowed to have a martensitic structure with more or less residual austenite that has maximum hardness of the GS cast irons [7].

Table 2 – HV30 Hardness of the materials

	F9	**GS**	**GS 4Cr**
	Before treatment		
HV30	471	366	554
	After treatment		
HV30	509	511	691

3.2.3. Observations

A first phase of this treatment (austenitization or heating) followed by maintenance made it possible to obtain homogeneous matrix, sufficiently loaded with carbon and a partial dissolution of carbides. The amount of carbon in the austenite matrix found in martensite has helped to regulate the hardness of the martensite and the maintenance time has only played the role of ensuring a uniform redistribution of carbon at all points of the piece [7]. As for the second phase, tempering, it allowed a relaxation of the constraints induced by quench heat treatment and in solution of a part of the carbides. For example, tetragonal martensite (α') releases carbon into oversaturation to produce depleted martensite and carbides. Hence a slight decrease in hardness on samples after tempering heat treatment.

3.3. Impact resistance of material

The results of these tests are given in Tables 4 and 5.

3.3.1. Raw casting material

In the raw casting state, the GS and GS 4Cr nuances have higher impact resistance values than 9 cast iron (Table 3).The high chromium content in 9 cast iron nuance would explain the low impact resistance of the 0.6 J/cm^2; Indeed, by reducing its content in nuance, the impact resistance of materials increases by a factor greater than 5.

3.3.2. Treated materials

After heat treatment, there is a considerable increase in impact resistance compared to the raw casting state of the developed materials.

Table 3 shows a significant increase in impact resistance values for GS and GS 4Cr nuances. The impact resistance of the treated 9 cast iron has certainly increased, but in ratio 5 remains nearly two others.

Table 3 – Impact resistance of materials

	F9	GS	GS 4Cr
	Before treatment		
E (J)	0.5	2.7	2.3
K (J/cm^2)	0.6	3.4	2.9
	After treatment		
E (J)	0.7	4.0	3.8
K (J/cm^2)	0.9	5.0	4.8

3.3.3. Observations

The considerable reduction of chromium in the material allows other elements, such as copper, to influence the material by providing plasticity. On the other hand; the presence of graphite in the nuances GS and GS 4Cr also reinforces the plasticity of the material. Teaincrease in ductility (impact resistance) in thermally treated materials could be explained on the one hand by the presence of copper and nickel whose CFC structure is twice as ductility as that of the CC structure of the ferrite. Tempering treatment relaxes multiple stresses due to sudden cooling of quench heat treatment and change of structure to martensite. It is the basis for the increase in the tenacity of the materials despite a slight decrease in hardness [16].

3.4.Materials wear

3.4.1. Untreated materials

The results of these tests are given in tables 4 and 5. In the raw casting state, only the GS and GS 4 Cr nuances were subject to wear test and mass losses are given in table 4 below:

Table 4 - Mass loss of raw samples by wear test

Time [min]	**Mass losses [g]**	
	GS grade	**GS 4Cr grade**
2	0.1993	0.1589
4	0.106	0.0744
6	0.1237	0.0096
8	0.0365	0.0019
10	0.0222	0.0081
12	0.0045	0.0029
14	0.0023	0.011
16	0.037	0.012

The GS cast iron showed an average loss of 0.066438 g during the GS 4Cr cast showed an average loss of 0.03485 g. The different CMD values obtained are given in table 5 below:

Table 5 - CMD Values of GS and GS 4Cr in raw casting state

Time [min]	**CMD GS grade**	**CMD GS 4Cr grade**
2	1,047	0.849
4	0.563	0.401

6	0.661	0.052
8	0.196	0.01
10	0.12	0.044
12	0.024	0.016
14	0.012	0.06
16	0.2	0.65

In the raw casting state, the GS nuance has a fast wear compared to that of the GS 4Cr cast; a material loss of 0.033 g/min for the GS nuance versus 0.017 g/min for the GS 4Cr. The high value of the GS nuance's wear speed could be explained by its low hardness value of all nuances in the raw state.

3.4.2 Treated materials

After heat treatments, loss of mass after wear test is given in figure 4 below:

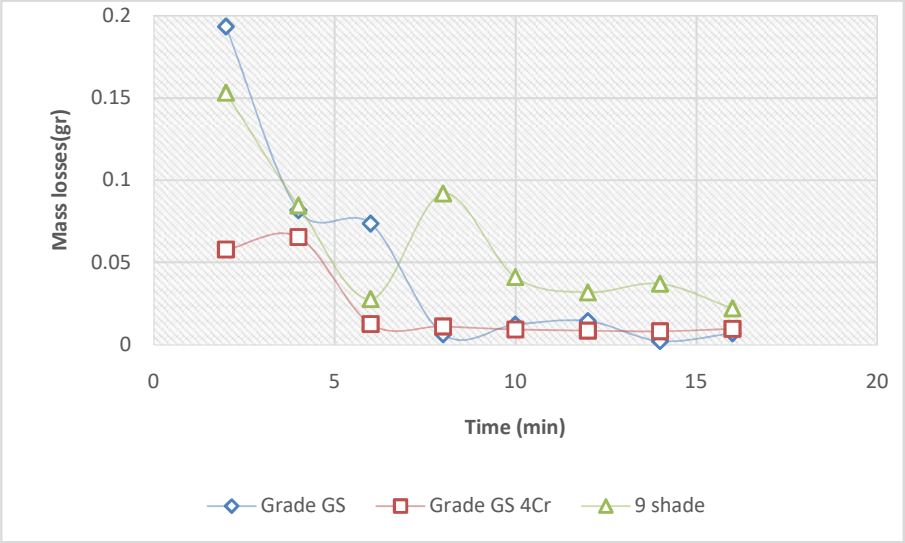

Figure 4 – Mass Losses by Tearing Samples After Heat Treatment

The different CMD values obtained are shown in figure 5 below.

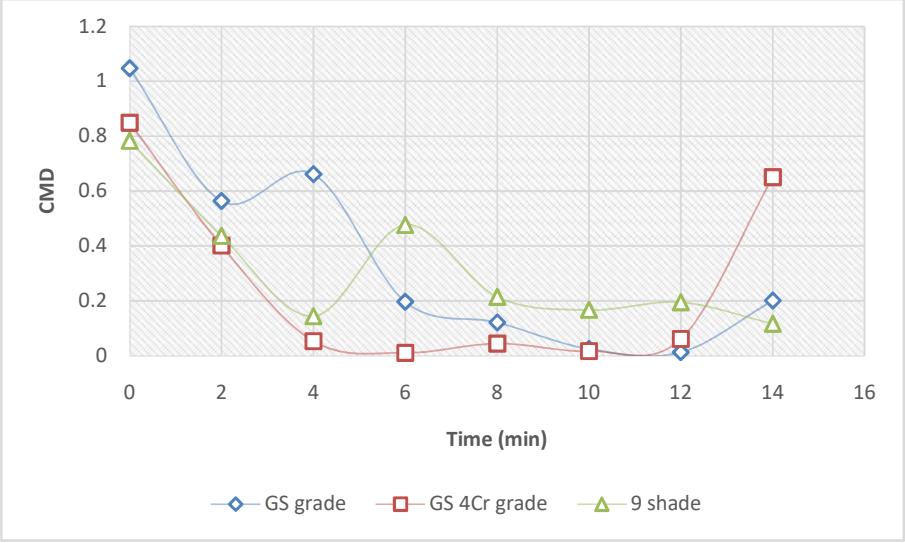

Figure 5 – CMD Values of GS, GS 4Cr and Cast 9 after thermal treatments

At the end of these results, the GS nuance wears out with a speed of 0.024 g/min, certainly slower than the 9 cast iron which wears out at 0.031 g /min; but its wear is still greater compared to that of the GS 4Cr nuance which revolves around 0.011 g/min. The decrease in material loss in the case of GS cast iron could be explained by a significant increase in hardness after quench heat treatment while normalization has led to a softening of 9 cast iron.

3.4.3. Observations

The wear of these nuances are intimately linked to their hardness. In both cases, the GS 4Cr nuance maintains a lower wear speed compared to other nuances.

The low wear of the chromium GS cast iron compared to that of the GS cast iron after same heat treatment could be explained by the difference in the chemical elements constituting these two materials. The chromium GS cast iron contains a large amount of chrome, at 4.5% while the GS cast iron contains only 0.3%. Chromium is the best element in enhancing the wear resistance of materials because of its ability to form extremely hard carbides that rush into the matrix instead of rushing to grain joints [4] [17].

3.6. Materials lifetime approximation

The hypothesis adopted to calculate the lifetime of materials is such that: knowing the volume of the sample as well as its mass, it is easy to determine the density of cast iron nuance. The geometric conditions of lifting bars being known, before and after use, their lifetime is approximately determined as a function of wear speed. Table 6 gives materials lifetime calculated for lifting bars produced according to each nuance [39].

Table 6 - Materials lifetime

	Sample mass (g)	Sample volume (mm^3)	Volumic mass (kg/m^3)	Lifting bar		Wear speed (g/min)	Lifetime (days)
				mass (kg)	*loss (kg)*		
F 9 treated	19.57	2730	7168.5	74.5	10.8	0.031	242
GS	19.03	2730	6970.7	72.6	10.5	0.033	220
GS treated	18.13	2730	6641.0	69.2	10.0	0.024	285
GS 4Cr	18.72	2730	6857.1	71.4	10.4	0.017	413
GS 4Cr treated	17.42	2730	6381.0	66.5	9.6	0.011	585

Observation

The obtained results on the determination of five materials lifetime that were the subject of our study guide the choice of material with optimal properties. Of all the nuances, cast iron GS 4Cr has the best lifetime with 413 and 585 days respectively for the raw casting material and the treated form. The latter form leads to a compromise between good properties and better lifetime.

4. Conclusion

The aim of this study was to develop a high performance material intended for the manufacture of molded parts subjected to wear and shocks, including the lifting bars of autogenous crushers. Thus, three types of materials were studied: cast iron 9, cast iron GS and cast iron GS with 4% chromium.

The metallographic study revealed several different structures in which is observed precipitation of an e ferritic-pearlitic structure containing nodules and graphite vermicules in the case of cast iron GS and

cast iron GS 4% Cr. After quench and tempering heat treatment, we have obtained a bainite coarse needles structure in austenitic-martensitic matrix accompanied by nodules and graphite vermicules for the cast iron GS nuance and a structure with austenitic-martensitic matrix accompanied by slats of eutectic carbides and the fine secondary carbides:$(Cr,Fe)_7C_3$ and $(Cr,Fe)_3$Ctypes, containing graphite nodules and vermicles. Exceptionally, for the case of cast iron 9 normalized, the precipitation of a proeutectoid carbide is observed around aggregates of fine perlite with a transformed ledeburite. Proeutecoid carbides are of$(Cr,Fe)_7C_3$ and $(Cr,Fe)_{23}C_6$ types.

After heat treatment, the microstructure of cast iron 4% Cr nuance contains secondary carbides of types$(Cr,Fe)_3C$ and $(Cr,Fe)_7C_3$ rich in chromium which give to this cast iron great hardness and good impact resistance than those of unalloyed GS cast iron.

Evaluation of the lifetime of different materials has shown that the best material to use for the manufacture of the lifting bars is GS cast iron 4% chrome quenched and tempered with a lifetime of 585 days.

To complete this resaerch, a study of the quantification of the volume of carbides can be carried out in order to highlight the influence of the total volume of car bides on the abrasion resistance of the materials.

Conflict of interest statement

On behalf of all authors, the corresponding author states that there is no conflict of interest

5. References

1. Kapend, J. 2019. Travail de fin d'études. *Substitution de la fonte fortement alliée au chrome par une fonte à graphite sphéroïdale martensitique*. Faculté Polytechnique de Likasi. Inédit. 70p.
2. Fillot, N. 2004. Thèse de doctorat. Etude mécanique de l'usure.*Modélisation par Eléments Discrets des débits de troisième corps solide*. Ecole doctorale des sciences appliquées. Lyon. 100p.
3. Archard, J. F. 1953. *Contact and rubbing of flat surfaces, Journal of Applied Physics*. pp 981-988.
4. Axéan, N. Hogmark, S. 1994. *Influence of hardness of the counterbody in three-body abrasive wear-an overlooked hardness effet*. Tribology International, N°27, p. 233-241.
5. Welding, D. Alloys, G. 2016. Dursteel. *Aciers et composants anti-usure*. 10p. info@wa-produr.com.
6. Mezlini, S. 2003.These de doctorat. *Etude de l'usure par abrasion d'alliages d'aluminium*. Ecole Centrale de Lyon 24. pp 47-152.
7. Mounir SAHLI, 2013. Projet de fin d'étude. *Effet des traitements thermiques sur la microstructure d'une fonte fortement allié au chrome utilisé pour la fabrication des boulets de broyage*. Université Mentouri. Constantine. 86p.
8. Leonardo, D.V. 2015. Fonderie Acciairie Roiale. *Fonte blanche à haut chrome*. 33010 Reana del Rojale (Ud) Italia. www.farspa.com.
9. El Bied, N. 2015. Projet de fin d'études. *Développement de deux nuances de la fonte à haute teneur en chrome*. Faculté des sciences et techniques. FES. 93p.
10. Hervas Dobon, I. 2013. Thèse de doctorat. *Contribution à l'étude des mécanismes d'endommagement des fontes ferritiques à graphite sphéroïdal. Influence de la température, du trajet de chargement et rôle des interfaces nodulaires*. Université de Caen Basse-Normandie. Caen. 120p.

11. Jault, J. 2001. *Fontes à graphite sphéroïdal. Propriétés d'utilisation.* Techniques de l'ingénieur. Matériaux métalliques. pp 150-324.
12. Dierickx, P. 1996. Thèse de doctorat. *Etude de la microstructure et des mécanismes d'endommagement de fontes G.S. ductiles. Influence des traitements thermiques de ferritisation*. Lyon : Institut national des sciences appliquées de Lyon. 105p.
13. Rawen, J. 2017. Thèse de doctorat. *Caractérisation microstructurale du graphite sphéroïdal formé lors de la solidification et à l'état solide*.
14. Laplanche, H. 1976. *Les fontes et leurs traitements thermiques*. 1ere éd. Paris: PYC Edition Desforges. 80p.
15. Jacques, B. 2017. Thèse de doctorat. *Sphéroïdisation du graphite –cas de la fonte centrifugée*. Toulouse : Institut National Polytechnique de Toulouse (INP Toulouse). 150p.
16. Muriel, H. 2010. *Influence d'éléments d'addition sur les transformations de la martensite revenue dans les aciers faiblement alliés*. Ecole nationale supérieure des mines de Saint-Etienne. pp 50-100.https://tel.archives-ouvertes.fr/tel-00541049.
17. Subramanian, C. 1991. *Some considerations towards the design of a wear resistant aluminum alloy*. Londres. p. 193-205.
18. Le Gal, J. 2014. *Fontes à graphite vermiculaire (GV)*. Mise en forme des métaux et fonderie. (consulté le 6 mars 2019).
19. Bastid P et al. 1997. *Microstructural Evolution of Spheroidal Graphite Cast Iron at High Temperature: Consequences on Mechanical Behaviour*. Advanced Materials Research, p.139–146.
20. Borel, P.1986. *Propriétés des fontes à graphite nodulaire. Fontes à graphite sphéroïdal*. Techniques de l'ingénieur. Matériaux Métalliques. Paris. 392p.
21. Eyraud, T. *Tontes blanches*. E-monsite.com. (seen on July 28th, 2020).
22. Liu,Y. Rohatgi, P. 1991. *A map for wear mechanisms in aluminum alloys*. Journal of Materials Science, pp 99-102.
23. Markus, B. Conrad, M. 2015. *Kalenborn*. 32p. www.kalenborn.com.
24. Brazovla, G. 2012. *Metso*. AB, SE-934 81 Ersmark, Suede. www.metso.com.
25. Margerie J.C. 1989. *Propriétés des fontes grises ordinaires. Fontes à graphite lamellaire non alliées. Techniques de l'ingénieur*. Matériaux métalliques. Paris. N°380. 380p.
26. Lampman, S. 1996. *Fatigue and Fracture. In ASM International. A.S.M. International*. A.S.M. International Handbook. Londre. pp 1676-1717.
27. Loiselet, N. 2013. *Propriétés mécaniques des fontes GS*. pp 1-15.
28. Adrien J, 2004. Thèse de doctorat. *Optimisation des cycles thermiques appliqués aux fontes GS ferritiques vis à vis des propriétés de fatigue*. Ecole doctorale matériaux de Lyon. 120p.
29. Gonnet. 2003. *Article Résistance des matériaux*. Essais mécaniques.
30. Baralis, J. 1997. Précis de Métallurgie. *Elaboration, structure propriétés, normalisation*. 1ereedition, Afnor-Nathan, Paris. 232 p.
31. Bex, T. & Garreau G. 1992. *Les bases de l'inoculation. Hommes et fonderie*. N°224. pp33–37.
32. Bletry, M. 2007. *Méthodes de caractérisation mécanique des matériaux*. Extrait de Discorsie dimostrazioni mathematiche de Galilée. 9p.
33. Dautzenberg, J. H. Zaat, J. H. 1973. *Quantitative determination of deformation by sliding*. Wear, N°23. pp 9-19.
34. Mwema, M. (2018).*Cours de caractérisation des matériaux*. faculté polytechnique de Lubumbashi. Unilu. Inédit.
35. Nadot, Y. 1997. Thèse de doctorat. *Influence des défauts de fonderie sur la résistance à la fatigue d'une fonte GS*. Ecole nationale supérieure de mécanique et d'aérotechnique. Poitiers. Université de Poitiers. 110p.

36. Sersour, Z. 2010. Mémoire de magister : *Influence d'éléments d'addition sur les caractéristiques mécaniques et microstructurales des alliages Al-Si*. Ecole doctorale. Science et Ingénieur. Matériaux-Structure et Environnement. Bougara. pp 40-90.
37. Rémi, D. Raymond, L. 2015. Mémoire de magister. *Guide d'auto-apprentissage pour les opérateurs en traitement thermique*. Québec. 186p. ISBN 978-2-922946-17-8.
38. Mathieu, b. 2016. Thèse de doctorat. Contribution à l'étude et au développement de nouvelles poudres de fonte. Montreal. 186p.
39. Nadipuram, V. Jordi, M. Fuerst, A. 2019. L'apprentissage automatique surveille le blindage des broyeurs miniers. Système autonome, ABB Review. Suisse.